



Adsorption of indium and zinc ions from aqueous solutions by carboxymethyl chitosan/poly(acrylic acid) microbeads

Chen-Chia Huang*, Jeng-Jyun Huang

Department of Chemical and Materials Engineering, National Yunlin University of Science and Technology, 123 University Road, Section 3, Douliu, Yunlin 64002, Taiwan, ROC, Tel. +886-5-534-2601 Ext. 4616; Fax: +886-5-531-2071; emails: huangchc@yuntech.edu.tw (C.-C. Huang), M10115008@yuntech.edu.tw (J.-J. Huang)

Received 19 November 2017; Accepted 21 June 2018

ABSTRACT

This study prepared chitosan (CS), carboxymethyl chitosan (CMC), and carboxymethyl chitosan/poly(acrylic acid) (CMC/PAA) microbeads through suspension polymerization in order to investigate the indium adsorption properties onto these microbeads from aqueous solutions. The study further observed the morphology of the prepared microbeads by an optical microscope, characterizing the structure by Fourier transform infrared spectroscopy and measuring the point of surface zero charge by the pH drift method. The adsorption capacity was determined by batch adsorption techniques for indium and zinc ions from both single-solute and bisolutes solutions. The equilibrium data of a single solute (indium or zinc) adsorbed on the microbeads was best described by the Langmuir adsorption isotherm model. It is found that the maximum adsorption capacity of indium ion on the microbeads are in the order CMC/PAA > CMC > CS. The adsorption kinetics of indium on the microbeads best fits the pseudo-second-order model. According to thermodynamic analysis, the indium adsorption onto the microbeads was spontaneous, while the zinc adsorption was nonspontaneous. From the bisolutes' adsorption experiments, the microbeads exhibit good selectivity for indium metal ion. Through reusability studies, the microbeads still have good adsorption capacity for indium ions after five cycles of adsorption–desorption run.

Keywords: Adsorption; Chitosan; Carboxymethyl Chitosan; Poly(acrylic acid); Indium ion

1. Introduction

With the rapid development of the global optoelectronics industry, indium has become a key metal. Indium is mainly used for manufacturing liquid crystal display, semiconductors, thin-film transistors, thin-film solar cells, and fiber-optic communication elements [1]. Due to huge market demand, indium ore is mined in large quantities. However, the indium content is very low in the earth crust; it is not an independent mineral, and it is usually accompanied by zinc, tin, and lead minerals, with zinc ore having the highest indium content. At present, indium is extracted mostly from the zinc smelting slag byproduct, usually bring with it a lot of zinc constituent [1].

In addition, as the heavy metals in the wastewater from the photoelectric material and element manufacturing industry harm the environment and human health, Taiwan's environmental laws have specified the maximum indium discharge limit value in industrial effluent at 0.1 mg/L.

Based on sustainable utilization of resources and waste management, research on recovering indium from the waste of photovoltaic elements [2,3] and industrial effluent has become increasingly important [4,5]. Common indium recovery techniques include liquid-phase extraction [6,7], chemical precipitation [8], electrocoagulation recovery [9], and adsorptive separation [5,10–18]. The adsorptive separation technique is regarded as a recovery method with development potential, because of its low cost, good selectivity, and recoverability. The indium ion adsorbents are agriculture waste [10,11], silica gel [12], impregnated

* Corresponding author.

resins [13,14], ion exchange resins [15–17], and carbon nanotubes [18]. According to various documents, there is still room for breaking through the adsorbability for indium ions.

Chitosan (CS) is a low toxicity and biodegradable natural polysaccharide. It is a natural polymer material used in large quantities in recent years due to its low price and environmental friendliness. CS has a hydroxyl group and amine active functional group; it is capable of chelating, complexing, and electrostatic attraction of metal ions [19,20]. Studies have indicated that CS has a good adsorption effect on metal ions [21–25]. The active functional group in the CS structure can enhance the chemical characteristic of its structure by chemical modification; for example, the carboxymethyl functional group-modified CS has been used to adsorb metal ions, enhancing the adsorbability of the modified CS for metal ions [21,22]. The poly(acrylic acid) (PAA)-modified CS is likely to form an electrostatic effect on positively charged ions and has a good removal adsorption effect on metal ions [23–25].

This study prepared the carboxymethyl chitosan (CMC) by using a chemical modification, and then the CS, CMC, and CMC/PAA microbeads are prepared by using suspension polymerization. In the monocomponent indium and zinc metal ion systems, different pH values, adsorption isotherm, adsorption kinetics, and adsorption thermodynamics are tested, in order to discuss the adsorbability and adsorption behavior of particles. The selectivity of particles for indium ions is observed by bisolutes solution adsorption experiments.

2. Materials and experiments

2.1. Materials

Food grade CS was obtained from Charming and Beauty Co., Taiwan. Its weight-average molecular weight was 300–500 kDa, and the deacetylation degree was 90% as stated by the manufacturer. PAA with M.W. 100,000 and 35 wt.% in H₂O solution was obtained from Aldrich Co. (New York, USA). Glutaraldehyde with 25 wt.% in H₂O and chloroacetic acid (99%) were obtained from Acros Organics (Geel, Belgium). Methanol (99%), 2-propanol (99%), and hexane (95%) came from ECHO Chemicals Co. (Taiwan). Glacial acetic acid and Span 80 were purchased from Merck (Darmstadt, Germany). Anhydrous indium(III) chloride (99.99%) and zinc(II) chloride (99.99%) were obtained from Alfa Chemicals Ltd. (England). Hydrochloric acid, sodium hydroxide, acetic acid, and all other chemicals used in this research were of analytical reagent grade and were used without any further purification.

2.2. Preparation of microbeads

2.2.1. Preparation of CS

CS microbeads were prepared according to the procedure described in detail elsewhere [26]. In brief, 2 g of CS powder and 0.95 mL of acetic acid were dissolved in 80 mL of water. The solution was then dispersed evenly in 300 mL *n*-hexane containing a small amount of Span 80. Next, 2 mL glutaraldehyde solution was added dropwise. Subsequently, the cross-linking reaction was kept at 323 K for 1 h. After completion of the reaction, the mixture was neutralized by a diluted NaOH aqueous solution to pH approximately 9.0; the microsphere was then filtered from *n*-hexane and washed

with ethanol and distilled water. The filtered microbeads were dried at 333 K for 24 h and then stored in a desiccator for further use.

2.2.2. Preparation of CMC

CMC was synthesized via a method proposed by Mourya et al. [27]. Initially, 5 g CS was dispersed in isopropanol (50 mL). Next, 30 wt% NaOH aqueous solution was added dropwise under magnetic stirring at room temperature over a period of 30 min. After alkalization, 7 g chloroacetic acid dissolved in isopropanol was added under continuous stirring. The reaction mixture was stirred in a simple reflux reactor with a water bath at 333 K for 4 h. The solid product was then filtered, suspended in methanol, and neutralized with glacial acetic acid.

The CMC microbeads were prepared as follows [21]: CMC (2 g) was dissolved in 80 mL water, and then the solution was dispersed evenly in 300 mL *n*-hexane containing a small amount of Span 80. The following steps, cross-linking reaction by glutaraldehyde solution and washing step, have been prepared the same as before.

2.2.3. Preparation of CMC/PAA

The CMC/PAA microbeads were prepared in the similar manner proposed by Dai et al. [23]. In brief, 2 g of PAA was dissolved in 3 mL distilled water, and then was added into the CMC solution (2 g CMC was dissolved in 80 mL water). The following preparation process was the same as the CMC microbeads preparation.

2.3. Characterization

The shapes and morphology of the microbeads were observed by an optical microscope (OM). The structures of CS, CMC, and CMC/PAA were characterized using a Fourier transform infrared (FTIR) spectrometer (PerkinElmer Spectrum one). All samples were prepared as KBr tablets, and the range of tested wave numbers is 450–4,000 cm⁻¹. The pH at the point of zero charge (pH_{pzc}) of the microbeads was measured by using the pH drift method [28]. The pH of 0.01 M NaCl solution was adjusted to successive initial values between 2 and 12, by adding either HCl or NaOH. The optimum amount of microbeads (15 mg) was added in 15 mL of respective pH solution and left at room temperature for 48 h. After the pH stabilized, the final pH was measured. The graphs of pHs were drawn and used for the determination of points at which the initial and final pH values were equal.

2.4. Batch adsorption

Adsorption experiments for a single-metal system and stock solutions of indium and zinc ions were prepared by dissolving appropriate amounts of anhydrous InCl₃ and ZnCl₂ in distilled water, respectively. Working solutions ranging from 20 to 150 mg/L were prepared by diluting the stock solutions. For batch adsorption experiments, 100 mL solutions were added in 250 mL stopper conical flasks and shaken on a temperature controlled shaker at 80 rpm.

The initial pH values ranged from 2.0 to 4.0 and were adjusted by 0.1 M HCl or NaOH solutions. Adsorption equilibrium studies were carried out by contacting 15 mg microbeads with 100 mL of metal ions solution with different initial concentration (20–150 mg/L) in 250 mL stopper conical flasks. The mixtures were shaken at 303 K for 24 h. Kinetic experiments were carried out by contacting 100 mL In^{3+} and Zn^{2+} solution of an initial concentration of 30 mg/L with 15 mg adsorbents in 250 mL conical flasks at temperature 303 K and pH 4. Samples (2.0 mL) were taken at predetermined time intervals for the analysis of residual metal concentration in the aqueous solution. The concentration of each metal ion was determined with an atomic absorption spectrophotometer (PerkinElmer, AAnalyst 400). All the batch experiments were performed in triplicate, and the average data were used in data analysis.

To determine the adsorption characteristics of the microbeads in a binary metal mixture, the initial concentrations were conducted by two cases: one with both In and Zn ions of 20 mg/L, the other with 10 mg/L In ion and 50 mg/L of Zn ion. All the experiments for the binary system were conducted at pH 4, temperature 303 K, and adsorbent dose of 15 mg for 24 h. The concentrations of In and Zn were determined by an inductively coupled plasma spectrometer (PerkinElmer OPTIMA 5100DV).

The adsorption capacity at equilibrium (q_e , mg/g) was calculated by Eq. (1). For the kinetics study, the adsorption capacity at different adsorption times (q_t , mg/g) can be calculated by Eq. (2). The distribution coefficient (K_d) and selectivity (α) were calculated by Eqs. (3) and (4), respectively.

$$q_e = \frac{(C_o - C_e)}{m} \times V \quad (1)$$

$$q_t = \frac{C_o V - C_n (V - nv) - v \sum C_n}{m} \quad (2)$$

$$K_d = \frac{q_e}{C_e} \quad (3)$$

$$\alpha = \frac{K_d(\text{In})}{K_d(\text{Zn})} \quad (4)$$

where C_o and C_e are the initial and final equilibrium concentrations in the solution, respectively (mg/L); V is the initial

volume of solution (L); m (g) is the dry mass of the microbeads; C_n is the concentration of the n th sample solution (mg/L); and v is the sample volume (L).

After adsorbing metal ions from the solution of initial concentration 30 mg/L, at 303 K and pH 4 over 24 h, the adsorbents were regenerated with 0.1 M HCl 100 mL and then collected from the solutions by filtration and washed with distilled water. The regenerated microbeads were reused in the next cycle of adsorption experiments.

3. Results and discussion

3.1 Characterization

This study uses suspension polymerization to produce CS microbeads. The size of the beads is influenced by the droplet (dispersed phase) viscosity, the interfacial tension between dispersed phase and continuous phase, surfactant concentration, rotation speed, temperature, magnet rotor, and reaction vessel size [17]. In order to reduce the changes in the particle size and shape in the process, the aforesaid parameters were fixed to make particles. According to the optical photographs in Fig. 1, the three kinds of microbeads are approximately spherical, and their size is 10–25 μm .

Fig. 2 shows the FTIR spectra of obtained microbeads. The basic characteristic peaks of CS in all samples are located around as follows: the broad peaks about 3,100–3,500 cm^{-1} correspond to $-\text{OH}$ and $-\text{NH}$ stretching vibrations; the peak about 2,923–2,867 cm^{-1} is ascribed to $-\text{CH}$ stretching vibration; the peak about 1,590–1,650 cm^{-1} represents $-\text{NH}$ bending vibration in $-\text{NH}_2$; the peak at 1,154 cm^{-1} bridges $-\text{O}$ stretching; and the peak about 1,029–1,070 cm^{-1} is assigned to $-\text{CN}$ and $-\text{C}-\text{OH}$ stretching vibrations, respectively [23,27]. At 1,376 and 1,414 cm^{-1} , $\text{C}-\text{N}$ axial vibration and $\text{N}-\text{H}$ angular vibration absorption peaks [27] were observed, indicating that the microbeads cross-linked by glutaraldehyde still had the presence of amino structures. The above peaks are also observed in Figs. 2(b) and (d), showing that the CMC and the mixed PAA beads (CMC/PAA) still have the basic properties of the CS structure.

Since CMC and CMC/PAA were obtained by coprecipitation in NaOH solution, the carboxyl groups were deprotonized and formed Na-form beads, when even washed to neutral. For comparison, the blending beads were treated in acidic solution to be H-form ones before the FTIR measurement. The FTIR spectra of Na-form and H-form CMC and

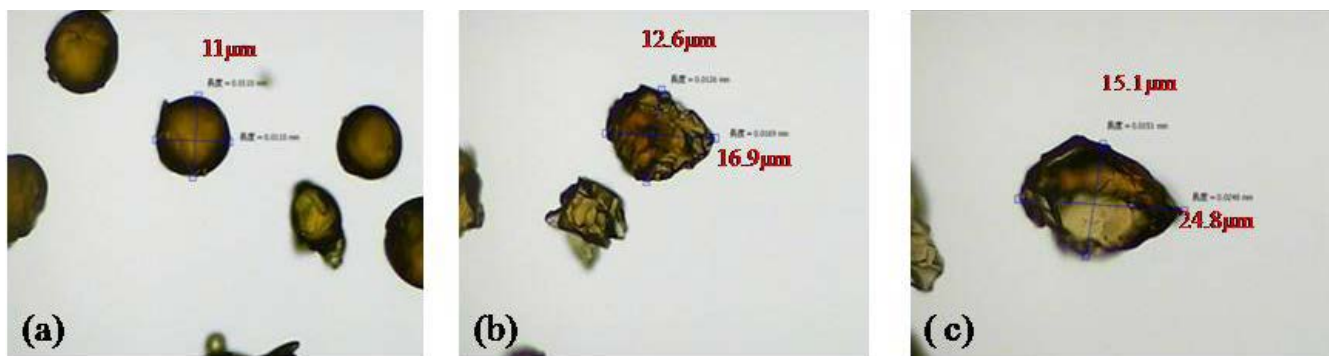


Fig. 1. Optical photographs of the microbeads (a) CS, (b) CMC, and (c) CMC/PAA.

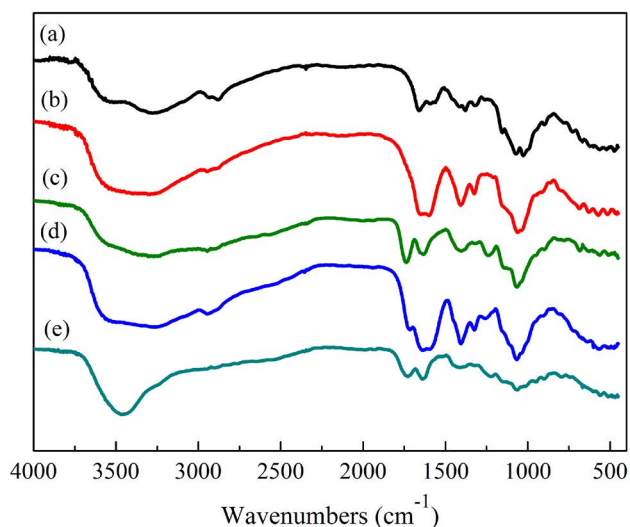


Fig. 2. FTIR spectra of the microbeads (a) CS, (b) CMC, (c) CMC-H, (d) CMC/PAA, and (e) CMC/PAA-H.

CMC/PAA beads are shown in Figs. 2(b) and (c) and (d) and (e), respectively. In the FTIR spectra of H-form of CMC and CMC/PAA, two new characteristic peaks appeared at 1,736 and 1,624 cm^{-1} , which were assigned to $-\text{COOH}$ and $-\text{NH}_3^+$, respectively. This indicates that PAA has been successfully blended in the CS microbeads.

The pH at which the charge of the solid surface is zero is referred to as the zero point of charge (pH_{zpc}). For the solution with pH values lower than pH_{zpc} , the active sites of the sorbent are protonated and have positive charge. However, at pH values higher than pH_{zpc} , the surface charge of the adsorbent is negative. Fig. 3 presents the results of the pH drift method for the determination of pH_{zpc} of the microbeads. It was found that pH_{zpc} of CS is equal to 8.72, which is located between literature values 7.8 and 9.9 [25,29,30]. CS has different pH_{zpc} values, which may be related to different material preparation methods and deacetylation

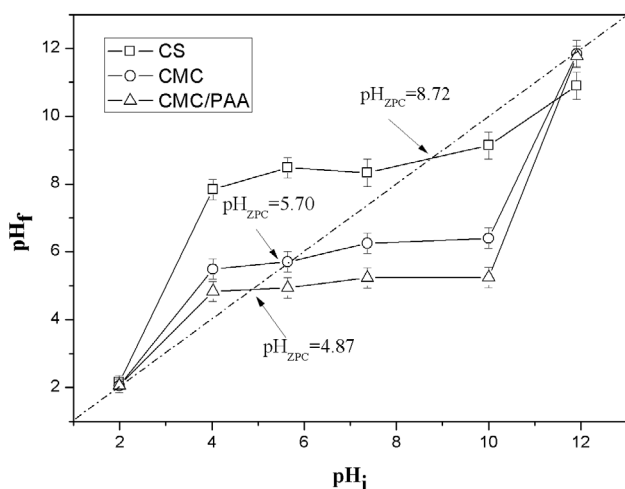


Fig. 3. pH_{zpc} determination by the pH drift method of the microbeads.

degrees [25]. The pH_{zpc} value of CMC is 5.70, lower than CS, because the CMC diaphysis is grafted with negatively charged carboxymethyl as a result of chemical modification, and the carboxymethyl and electropositivity in the structure cut down each other, thus decreasing pH_{zpc} . This result is very close to the CMC isoelectric point pH_{iep} 5.5 obtained by Ref. [29]. When CMC is mixed with PAA, the pH_{zpc} value decreases again, as PAA is a linear polymer with a carboxylic acid group, and its pK_a value is about 4.5 [31]. When forming an interpenetrating net polymer with CMC, as many carboxylic acid groups are imported, the cut down of electropositivity and electronegativity is more severe, and the pH_{zpc} value decreases to 4.87.

3.2. Effect of initial solution pH on adsorption of In(III) and Zn(II)

As the pH value of indium ion solution is higher than 4.5, there will be indium hydroxide precipitate [32]. In order to avoid the precipitate influencing the adsorbance correctness, the experimental range is selected as pH 2.0–4.0. Fig. 4 shows the effect of pH value on the adsorption capacity of indium and zinc ions on microbeads under the conditions of ion concentration 20 mg/L, solution volume 100 mL, particle weight 15 mg, and temperature 303 K. Fig. 4 shows when the pH value is 2, that In^{3+} or Zn^{2+} has few adsorption capacity. The adsorption capacity increases with the pH of the solution. Because the indium and zinc ions exist as positively charged ions in solution [32,33], the hydrogen ion and positively charged metal ion form a competitive adsorption between activated adsorption sites. When the pH is low, the hydrogen ion concentration in the solution is high, and the competitive advantage is strong, so that the adsorption capacity of metal ions is low. When the solution pH is increased, the hydrogen ion concentration decreases relatively, so that the adsorption capacity of indium and zinc metal ions is relatively increased.

As shown in Fig. 4, the adsorption capacity on microbeads is maximized at pH 4, and the adsorbance order of two metal ions is CMC/PAA > CMC > CS. This can be explained by the pH_{zpc} of microbeads; when the solution $\text{pH} < \text{pH}_{\text{zpc}}$, the material surface tends to be positively charged, which is

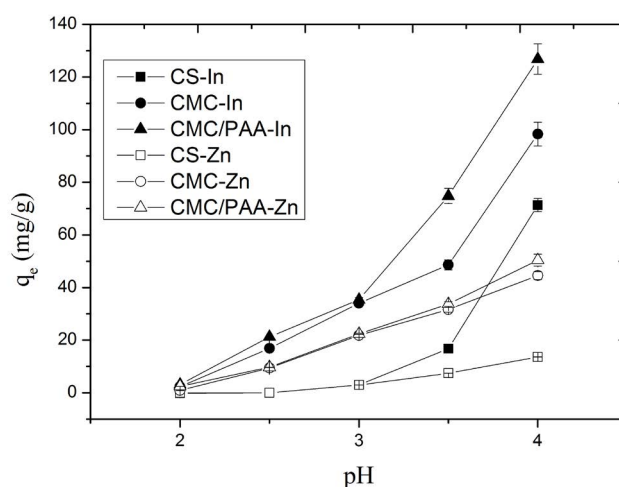


Fig. 4. Effect of initial solution pH on the adsorption capacity of In and Zn onto the microbeads.

adverse to positively charged metal ion adsorption. In other words, if the material has higher pH_{pzc} , then the surface has higher electropositivity and is more adverse to attracting positively charged ions. As mentioned earlier, the descending order of pH_{pzc} of microbeads is $\text{CS} > \text{CMC} > \text{CMC/PAA}$, meaning in low pH solution, the order of electropositivity of particles is the same, and so the order of cation adsorbance is $\text{CMC/PAA} > \text{CMC} > \text{CS}$. When $\text{pH} = 4$, the adsorption capacity of indium ions increases greatly, especially on CMC/PAA particles. Because $\text{pH}_{\text{pzc}} = 4.87$ of CMC/PAA, when the pH value of the solution increases from 3 to 4, the $-\text{COOH}$ functional group on the CMC/PAA surface is dissociated into the $-\text{COO}^-$ functional group; there is a strong attractive force between In^{3+} and CMC/PAA microbeads under the electrostatic effect, greatly increasing the adsorption capacity.

Fig. 4 shows that when the pH is high, the adsorption capacity of indium ion is higher than that of zinc ion, because the microbeads adsorb the positively charged ions in the solution by electrostatic attraction, and the metal with higher ionic valence has stronger electrostatic attraction power. The indium metal ion is trivalent, and the zinc metal ion is bivalent. Thus, the microbeads have better adsorbability for indium ions than for zinc ions [34].

3.3. Adsorption isotherms

Fig. 5 shows the isothermal equilibrium adsorption capacity of CS, CMC, and CMC/PAA for indium and zinc metal ions at $\text{pH} = 4$ and 303 K. As mentioned earlier, the adsorption isotherms of CS, CMC, and CMC/PAA for indium ion is far larger than that for zinc ion.

The Langmuir [35] and Freundlich [36] isotherm models have widely been used in adsorption isotherm studies and were also used in this work to fit the experimental isotherm data for indium and zinc ions adsorption on CS, CMC, and CMC/PAA microbeads. The Langmuir and Freundlich isotherm models are represented by the following equations:

Langmuir isotherm:

$$q_e = \frac{q_m K_L C_e}{1 + K_L C_e} \quad (5)$$

Freundlich isotherm:

$$q_e = K_F C_e^{1/n} \quad (6)$$

where C_e is the equilibrium metal ions' concentration in the solution (mg/L); q_e is the equilibrium concentration on the

adsorbent (mg/g); q_m is the monolayer capacity of the adsorbent (mg/g); K_L is the Langmuir constant (L/mg) and related to the free energy of adsorption; K_F is the Freundlich constant $((\text{mg/g})(\text{L/mg})^{1/n})$; and n is the heterogeneity factor.

The fittings of the Langmuir and Freundlich isotherm models to the experimental isotherm data for indium and zinc ions' adsorption on CS, CMC, and CMC/PAA are also shown in Fig. 5. The parameters obtained are all listed in Table 1. Based on Table 1, the correlation coefficients (R^2) of the linear form for the Langmuir model are much closer to 1.0 than those of the Freundlich model. According to the Langmuir isotherm model parameter q_m value, the order of monolayer adsorption capacity of microbeads for indium metal ion is $\text{CMC/PAA} > \text{CMC} > \text{CS}$. The q_m values of all three kinds of microbeads are higher than 160 mg/g, and CMC/PAA is 214.6 mg/g. According to Refs. [19,20,37], the hydroxyl and amine in the CS structure are capable of complexing, chelating, and electrostatic attraction of heavy metal ions. The nitrogen atom of amine has an unshared electron pair, forming coordination complexing with metal ions, which is the main bonding position of CS and metal ions. A part of hydroxyl can take part in the coordination complexing of metal ions by proton abstraction. After carboxymethyl grafting, as the structure has additional electronegative functional groups, besides the original chelating complexing mechanism, there is an electrostatic attraction power between ions and the particle structure, so that CMC has a better adsorption performance than CS.

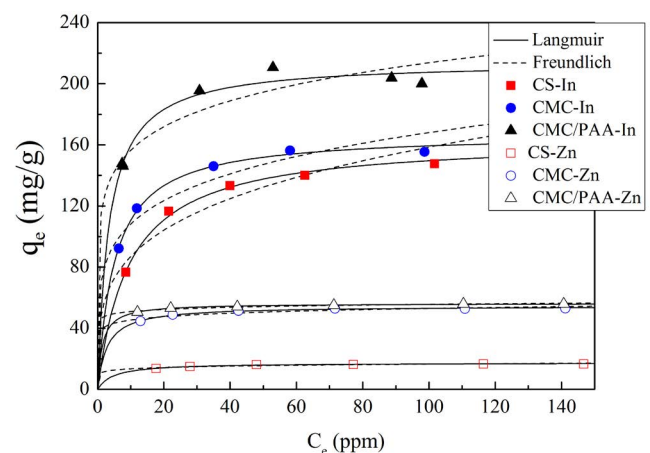


Fig. 5. Adsorption isotherms for In and Zn onto the microbeads ($\text{pH} = 4$, $T = 303$ K).

Table 1
Langmuir and Freundlich isotherm parameters for single metal ion adsorption at 303 K and pH 4.0

| Adsorbents | Metal | Langmuir | | | Freundlich | | |
|------------|-------|--------------|--------------|-------|------------|-----------------------------|-------|
| | | q_m (mg/g) | K_L (L/mg) | R^2 | n | K_F (mg/g)(L/mg) $^{1/n}$ | R^2 |
| CS | In | 163.9 | 0.104 | 0.99 | 3.83 | 47.67 | 0.87 |
| CMC | In | 167.5 | 0.194 | 0.99 | 5.23 | 69.67 | 0.88 |
| CMC/PAA | In | 214.6 | 0.291 | 0.97 | 7.38 | 114.57 | 0.85 |
| CS | Zn | 17.4 | 0.212 | 0.97 | 11.19 | 10.95 | 0.81 |
| CMC | Zn | 54.4 | 0.361 | 0.98 | 14.98 | 38.91 | 0.80 |
| CMC/PAA | Zn | 56.3 | 0.731 | 0.98 | 25.63 | 46.48 | 0.93 |

In addition, when CMC is mixed with PAA, the adsorption capacity is increased greatly, and the indium ion adsorbance is increased to about 1.28 times of CMC. Because PAA is an electronegative material, after it is mixed with particles, the surface zero potential of the structure is further reduced (as mentioned earlier), the electrostatic attraction power for cations is enhanced, and the carboxylic acid group of PAA and the metal ions can form chelate complex, increasing the adsorption capacity [23]. Furthermore, the q_m of indium ion adsorbed on all three kinds of microbeads is larger than that of zinc ion.

Table 2 lists the indium ion adsorption capacity of different adsorbents. The microbeads prepared in this study exhibit excellent indium ion adsorbability.

3.4. Adsorption kinetics

Adsorption kinetics discusses the mechanisms of the adsorption process. The general adsorption process mechanisms include external diffusion, intraparticle diffusion, and/or chemical reaction. The models for describing adsorption kinetics are divided into two main classes: reaction kinetics and diffusion models [33]. The surface of three kinds of microbeads is rough with a few pores and the metal ion adsorption mechanisms are mostly including chelating and electrostatic attraction. Thus, the reaction kinetics model is selected to regress the adsorption kinetics data. The common reaction kinetics models present pseudo-first-order and pseudo-second-order. Pseudo-first-order and pseudo-second-order models are generally expressed as Eqs. (7) [41] and (8) [42], respectively.

$$\ln(q_e - q_t) = \ln q_e - k_1 t \quad (7)$$

$$\frac{t}{q_t} = \frac{1}{k_2 q_e^2} + \frac{t}{q_e} \quad (8)$$

$$h = k_2 q_e^2 \quad (9)$$

Table 2
Indium uptake capacity of different adsorbents

| Adsorbent | pH | q_m (mg/g) | Reference |
|-----------------------------|-----|--------------|---------------|
| Chitosan/bentonite beads | 4 | 17.89 | [5] |
| Tea waste | 4 | 62.83 | [11] |
| D4DCHPA/resin | 2.4 | 25.25 | [13] |
| MSIRs | 3.0 | 58.75 | [14] |
| Calix[4]arene resin | 3 | 109 | [15] |
| Calix[6]arene resin | 3 | 213 | [15] |
| Poly(N-isopropylacrylamide) | 2 | 98 | [16] |
| Poly(VPA-co-MAA) | 6 | 80.37 | [17] |
| PAN/Amberlite XAD-2 | 6.5 | 13.5 | [38] |
| P507 extraction resin | 2 | 47.2 | [39] |
| EHEHPA/CSIRs | 1.5 | 23.8 | [40] |
| CS | 4 | 163.9 | Present study |
| CMC | 4 | 167.5 | Present study |
| CMC/PAA | 4 | 214.6 | Present study |

where q_t is the adsorption capacity at a certain time (mg/g); q_e is the equilibrium adsorption capacity (mg/g); and k_1 and k_2 are the respective adsorption rate constants of the pseudo-first-order kinetic model (h^{-1}) and pseudo-second-order kinetic model (g/mg/h), respectively. The h is the initial sorption rate (mg/g/h).

The adsorption kinetics of CS, CMC, and CMC/PAA for indium and zinc ions was carried out at 303 K, pH 4.0, and low initial concentration of 30 mg/L. The kinetic adsorption results are all shown in Fig. 6. From Fig. 6, the adsorption amount of metal ions increased rapidly during the first hour and then increased slowly. Malamis and Katsou [33] reported that at low metal concentration, the adsorbent surface coverage is low and the formation of surface complexes is the main mechanism. The increase of initial concentration results in an increase of adsorption capacity. The kinetics data in Fig. 6 are derived from low initial concentration, and the adsorbance is not yet saturated. Table 3 lists the match parameter values of pseudo-first-order and pseudo-second-order kinetic models. As shown in Table 3, the R^2 value and q_e value of the pseudo-second-order adsorption kinetic model are close to the experimental value q_e^{exp} , meaning this model is suitable for fitting the adsorption kinetic behavior of particles for the two metal ions. It is worthy to note that the initial sorption rate of indium ion on the microbeads is faster than that of zinc ion, except for CMC/PAA.

3.5. Thermodynamics of adsorption

In order to understand the heat of adsorption, and whether the process tends to be spontaneous, the study was carried out at temperatures of 303, 313, and 323 K. The thermodynamic parameters of the adsorption process, Gibbs free energy (ΔG°), enthalpy (ΔH°), and entropy (ΔS°) were calculated using the following equations [17,43]:

$$\Delta G^\circ = -RT \ln K_d \quad (10)$$

$$\ln K_d = \frac{\Delta S^\circ}{R} - \frac{\Delta H^\circ}{RT} \quad (11)$$

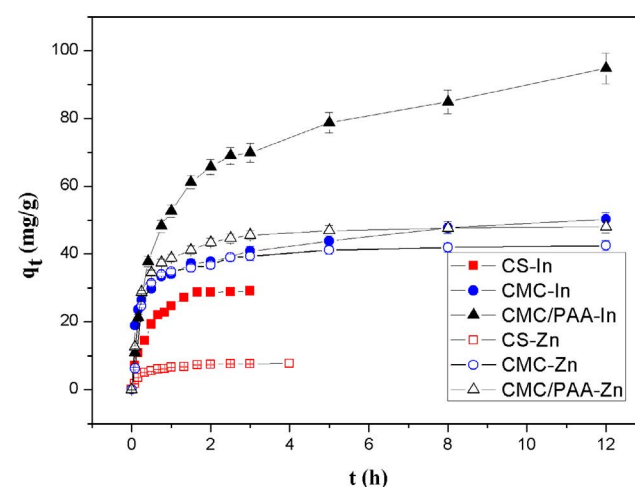


Fig. 6. Kinetic adsorption results of In and Zn onto the microbeads (pH = 4, $T = 303$ K, $C_0 = 30$ mg/L).

Table 3
Kinetic parameters for the single solute adsorption onto the different microbeads at 303 K, pH 4.0 and $C_0 = 30$ mg/L

| Adsorbent | Metal | Pseudo-first-order | | | | Pseudo-second-order | | | |
|-----------|-------|---------------------------|--------------|---------------------------|-------|---------------------|----------------|--------------|-------|
| | | q_e^{exp} (mg/g) | q_e (mg/g) | k_1 (h^{-1}) | R^2 | q_e (mg/g) | k_2 (g/mg/h) | h (mg/g/h) | R^2 |
| CS | In | 29.05 | 25.34 | 1.877 | 0.94 | 32.82 | 0.091 | 98.0 | 0.99 |
| CMC | In | 50.31 | 37.38 | 0.559 | 0.85 | 50.40 | 0.052 | 132.1 | 0.99 |
| CMC/PAA | In | 94.76 | 68.03 | 0.271 | 0.94 | 96.33 | 0.013 | 120.6 | 0.99 |
| CS | Zn | 7.68 | 5.138 | 1.413 | 0.97 | 8.10 | 0.597 | 39.2 | 0.99 |
| CMC | Zn | 42.67 | 19.02 | 0.528 | 0.94 | 44.24 | 0.045 | 88.3 | 0.99 |
| CMC/PAA | Zn | 48.05 | 21.52 | 0.597 | 0.95 | 48.80 | 0.101 | 240.5 | 0.99 |

where R is the universal gas constant (8.314 J/mol/K) and T is the absolute temperature (K). The plot of $\ln K_d$ versus $1/T$ gives the straight line from which ΔH° and ΔS° are estimated from the slope and intercept of the linear line, respectively. The ΔG° values at different temperatures were calculated using Eq. (10).

Table 4 lists the values of the thermodynamic parameters of indium and zinc ions adsorbed on the microbeads. According to the thermodynamic rule, the negative ΔG° values at given temperatures indicate the spontaneous nature of the adsorption and confirm the feasibility of the adsorption process. The positive ΔG° values indicate the nonspontaneous process. For indium ions adsorbed on all the microbeads, from Table 4, the negative values of ΔG° are found to be from -33.1 to -38.6 kJ/mol in the range of 303–323 K. This indicates that the indium ions' adsorption process is spontaneous. In general, a value of energy ΔG° in-between 0 and -20 kJ/mol is consistent with electrostatic interaction between adsorption sites and the adsorbing ion (physical adsorption), while a more negative ΔG° value ranging from -80 to -400 kJ/mol indicates that the adsorption involves charge sharing or transferring from the adsorbent surface to the adsorbing ion to form a coordinate bond [44]. Thus, based on the values of ΔG° , the adsorption of indium ions onto the microbeads may involve both physisorption and electrostatic attractive force. The magnitude of ΔH° is usually employed to classify physisorption and chemisorption. Ma et al. [45] reported that the ΔH° of physisorption (including van der Waals force, electrostatic force) is smaller than 40 kJ/mol. The positive ΔH° value implies that the adsorption is endothermic, which is also supported by the study for the temperature effect. The enthalpy change values are listed in Table 4 at around

5–15 kJ/mol, indicating physisorption during the adsorption process. From Table 4, the positive value of ΔS° indicates that randomness at the solid/solution interface increased during the adsorption process.

3.6. Adsorption selectivity of indium

Fig. 7 shows the comparison of the adsorption capacities of indium and zinc ions onto three kinds of microbeads in single adsorbate and biadsorbates systems. As mentioned before, the adsorption capacity of indium and zinc onto the microbeads still increases with the pH value of solution in the bisolutes system. From Fig. 7 it can be seen that the adsorption capacity of indium and zinc in the bisolutes system is lower than that in the single-solute system. This can be attributed to the fact that the active sites of the microbeads are simultaneously available for adsorption of indium and zinc ions. At pH 4, due to the increase of negative charge of the microbeads, the competitiveness between the two metal cations is relatively increased, and the adsorption capacity in the bisolutes system is significantly lower than that in single-solute system.

To discuss the indium metal ion adsorption selectivity (α) under different pH values, both the same and different initial concentrations of indium and zinc metal ions were used. At the same initial concentration, as shown in Fig. 8(a), the α value of CS is about 0.47 when the pH value is 2, and the α value is greater than 2 when the pH is 3. According to the monocomponent adsorption experiments (Fig. 4), CS has a worse adsorption performance on indium and zinc ions when the pH value is lower than 3; because CS has higher pH_{pzc} , the metal ion adsorption capacity is significantly

Table 4
Thermodynamic parameters for single-solute adsorption on the different microbeads

| Adsorbents | Metal | ΔG° (kJ/mol) | | | ΔH° (kJ/mol) | ΔS° (J/mol K) |
|------------|-------|---------------------------|-------|-------|---------------------------|----------------------------|
| | | 303 K | 313 K | 323 K | | |
| CS | In | -33.1 | -33.7 | -34.3 | 14.83 | 60.14 |
| CMC | In | -37.2 | -37.9 | -38.6 | 15.88 | 70.35 |
| CMC/PAA | In | -33.3 | -33.9 | -34.6 | 12.18 | 69.51 |
| CS | Zn | 2.12 | 1.73 | 1.39 | 13.21 | 36.69 |
| CMC | Zn | -2.15 | -2.36 | -2.64 | 5.29 | 24.53 |
| CMC/PAA | Zn | -2.31 | -2.6 | -2.84 | 5.87 | 27.02 |

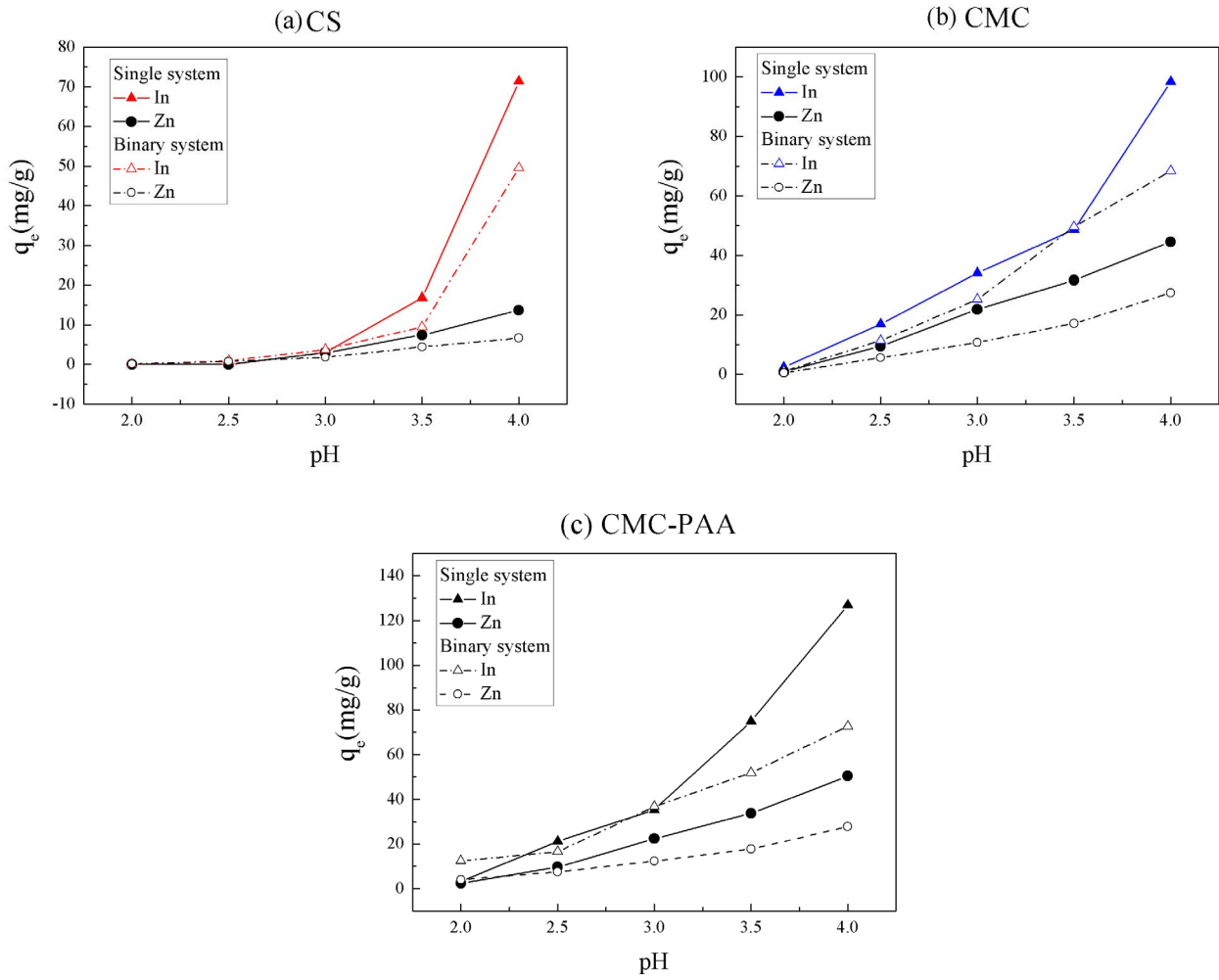


Fig. 7. Comparison of adsorption capacities of In (\blacktriangle , \triangle) and Zn (\bullet , \circ) onto the microbeads in single solute (full mark) and bisolutes (open mark) systems ($T = 303\text{ K}$, $C_0 = 20\text{ mg/L}$).

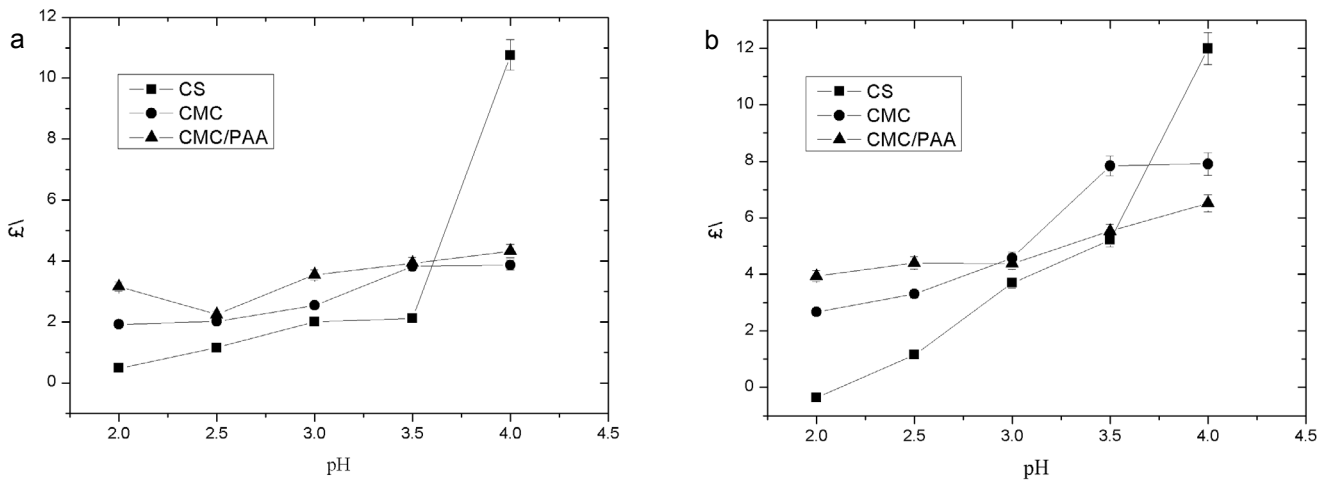


Fig. 8. Effect of initial solution pH on the selectivity of In adsorption from bisolute systems at 303 K: (a) In: 20 mg/L, Zn: 20 mg/L and (b) In: 10 mg/L, Zn: 50 mg/L.

increased only if the pH is high. When the pH is 4, the monocomponent adsorption experiment shows that the indium ion adsorption capacity of CS is enhanced significantly, and the zinc ion adsorbance is increased, but there is no significant change that increases the α value greatly. CMC and CMC/PAA have similar trends of selectivity for indium ion. Except for CS at pH = 2, α is greater than 1 under various pH values, meaning CMC and CMC/PAA have better adsorption capacities for indium ion than for zinc ion. This can be attributed to indium ion has more valence electron. As discussed earlier, the affinity between cations and microbeads depends on the valence electron structure of the metal ion. A similar result was reported by Wang et al. [34]. From the above regression results of adsorption isotherm model and kinetic model, indium ions have a higher saturated adsorption capacity and a faster initial adsorption rate. This result confirms the good selectivity of the microbeads for indium ions.

In the high zinc ion concentration and low indium ion concentration solutions, according to Fig. 8(b), the selectivity trend of various microbeads for indium ion is similar to the result of the same initial concentration, meaning the adsorption behavior changes slightly. Generally speaking, a high concentration adsorbate has a larger mass transfer driving force; when the adsorbent has not reached saturation adsorption, the mass transfer rate is high. Under the cases of high zinc ion concentration and low indium ion concentration, the α values of various microbeads are larger than that in Fig. 8(a), meaning the microbeads have excellent selectivity for indium ion; the sorption extraction effect is good, though, at low indium ion and high zinc ion concentrations.

3.7. Reusability study

In order to meet the economic benefit from reducing the processing cost and discharge of waste materials, the recycling of the adsorbent is the key point for evaluation. Fig. 9 shows the adsorption capacity of five adsorption–desorption

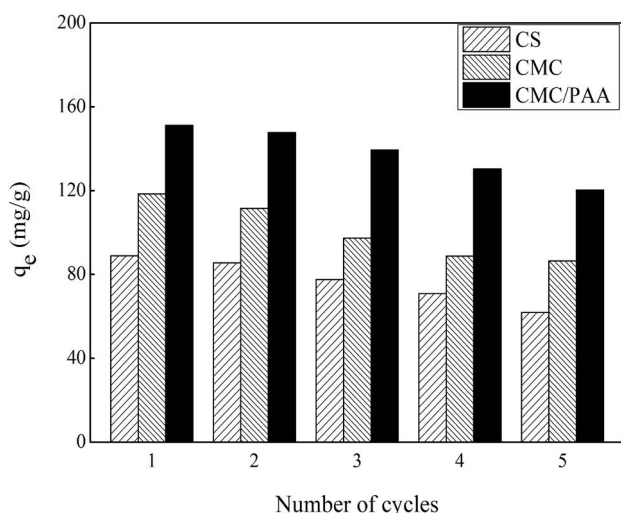


Fig. 9. Adsorption capacities of In on CS, CMC, and CMC/PAA microbeads after adsorption–desorption cycle operations.

cycle operations in which CS, CMC, and CMC/PAA adsorb indium ion, are desorbed by 0.1 M HCl solution, and then the indium ion is adsorbed. As shown in Fig. 9, the indium ion adsorption capacity of various microbeads decreases slightly as the cycle index increases perhaps because the desorbed microbeads not disengaged completely as a part of adsorption active sites are occupied by indium ions; and in the repetitive operation process, a part of the particles is left on the filter paper, resulting in losses, so that the adsorption capacity decreases slightly as the frequency of reuse increases. According to Fig. 9, after five cycle operations, the indium ion adsorption capacity of CS, CMC, and CMC/PAA is still 70%–80%, and the adsorption effect is still good compared with the equilibrium adsorption capacity of various references in Table 2. Therefore, the CS, CMC, and CMC/PAA particles have good adsorbability and reuse potential for indium ion.

4. Conclusions

This study uses suspension polymerization to prepare CS and CS-derivative microbeads. The particle size observed through OM is 10–25 μm . Here, FTIR proves that the particles still have amine after cross-linking, and the CMC and CMC/PAA structures contain a carboxylic acid functional group. According to the results of the drift pH method, the carboxylic acid group in the particle structure increases the electronegativity of the structure and reduces the pH_{pzc} . The adsorbability of microbeads for indium and zinc ions was tested, and besides chelation, the metal ions in solution are adsorbed by electrostatic attraction. The In(III) valence number is higher than Zn(II), and the indium ion adsorption effect is better when $\text{pH} = 4$. According to the monocomponent adsorption isotherm results of indium and zinc ions, the microbeads adsorption behavior inclines toward the Langmuir adsorption mode, and the order of saturation adsorption quantity q_m of indium ion is $\text{CMC/PAA} > \text{CMC} > \text{CS}$, meaning the carboxymethyl-modified and PAA-mixed microbeads can enhance the metal ion adsorbability. Based on the analysis of correlation coefficients, it is indicated that the pseudo-second-order kinetic model is better to describe the adsorption kinetics.

According to the results of thermodynamic analysis, the indium ion adsorption on particles at temperature 303–323 K tends to be spontaneous, the adsorption of zinc ion on CMC and CMC/PAA tends to be spontaneous, and CS tends to be nonspontaneous. The ΔS° and ΔH° are positive values, meaning there is a certain disorder in the solid–liquid interface; it is the heat absorption process, and the temperature rise is favorable for adsorption. The selective adsorption experiment on two-component indium ion shows that under the same ion concentration, the α value of various particles increases with pH, and the α values of CMC and CMC/PAA are greater than 1. The α value of CS is 11 when the pH is 4, meaning the particles have good selectivity for indium ion. The selective adsorption experiments at different concentrations indicate that the α value increases with the pH value, meaning a high zinc ion concentration solution is still favorable for the extraction separation of indium ion. The experimental results of microbeads reuse show that the indium ion adsorption capacity of particles decreases slightly as the cycle

index increases. Moreover, the adsorption capacity is still 70%–80% after five adsorption–desorption cycles, meaning the microbeads have good reusability.

Acknowledgment

This work was financially supported by the Ministry of Science and Technology, R.O.C. under grant no. MOST 103-2221-E-224-072.

References

- [1] A.M. Alfantatazi, R.R. Moskalyk, Processing of indium: a review, *Miner. Eng.*, 16 (2003) 687–694.
- [2] K. Takahashi, A. Sasaki, G. Dabdiba, N.S. Sadaki, T. Fujita, Recovering indium from the liquid crystal display of discarded cellular phones by means of chloride-induced vaporization at relative low temperature, *Metall. Mater. Trans.*, 40A (2009) 891–900.
- [3] A.V.M. Silverira, M.S. Fuchs, D.K. Pinheiro, E.H. Tababe, D.A. Bertuol, Recovery of indium from LCD screens of discarded cell phones, *Waste Manage.*, 45 (2015) 334–342.
- [4] J. Guan, S. Wang, H. Ren, Y. Guo, H. Yuan, X. Yan, J. Guo, W. Gu, R. Su, B. Liang, G. Gao, Y. Zhou, J. Xu, Z. Guo, Indium recovery from waste liquid crystal displays by polyvinyl chloride waste, *R. Soc. Chem. Adv.*, 5 (2015) 102836–102843.
- [5] M.J.C. Calagui, D.B. Senoro, C.C. Kan, J.W.L. Salvacion, C.M. Futralan, M.W. Wan, Adsorption of indium (III) ions from aqueous solution using chitosan-coated bentonite beads, *J. Hazard. Mater.*, 277 (2014) 120–126.
- [6] M.S. Lee, J.G. Ahn, W.C. Lee, Solvent extraction separation of indium and gallium from sulphate solutions using D2EHPA, *Hydrometallurgy*, 63 (2002) 269–276.
- [7] S. Virolainen, D. Ibane, E. Paatero, Recovery of indium from indium tin oxide by solvent extraction, *Hydrometallurgy*, 107 (2011) 56–61.
- [8] K.N. Han, S. Kondoju, K. Park, H. Kang, recovery of indium from indium/tin oxides scrap by chemical precipitation, *Geosyst. Eng.*, 5 (2002) 93–98.
- [9] W.L. Chou, C.T. Wang, K.Y. Huang, Effect of operating parameters on indium (III) ion removal by iron electrocoagulation and evaluation of specific energy consumption, *J. Hazard. Mater.*, 167 (2009) 467–474.
- [10] W.L. Chou, C.T. Wang, K.Y. Huang, Y.C. Chang, C.M. Shu, Investigation of indium ions removal from aqueous solutions using spent coffee grounds, *Int. J. Phys. Sci.*, 7 (2012) 2445–2454.
- [11] W.L. Chou, L.S. Chen, Y.H. Huang, C.Y. Huang, Effect of process parameters on the removal of indium ions from aqueous solutions by adsorption onto tea waste, *Fresenius Environ. Bull.*, 20 (2011) 603–610.
- [12] A. Tong, Y. Akama, S. Tanaka, Preconcentration of indium with 1-phenyl-3-methyl-4-stearyl-5-pyrazolone on silica gel, *Anal. Chim. Acta*, 230 (1990) 175–177.
- [13] T. Nakamura, T. Ikawa, S. Nishihama, K. Yoshizuka, Selective recovery of indium from acid sulfate media with solvent impregnated resin of bis(4-cyclohexylcyclohexyl) phosphoric acid as an extractant, *Ion Exch. Lett.*, 2 (2009) 22–26.
- [14] H. Li, J. Liu, X. Gao, C. Liu, L. Guo, S. Zhang, X. Liu, C. Liu, Adsorption behavior of indium(III) on modified solvent impregnated resins (MSIRs) containing sec-octylphenoxy acetic acid, *Hydrometallurgy*, 121–124 (2012) 60–67.
- [15] B.B. Adhikari, M. Gurung, H. Kawakita, K. Ohto, Solid phase extraction, preconcentration and separation of indium with methylene crosslinked calix[4]- and calix[6]arene carboxylic acid resins, *Chem. Eng. Sci.*, 78 (2012) 144–154.
- [16] H. Tokuyama, T. Iwama, Solid-phase extraction of indium (III) ions onto thermosensitive poly(N-isopropylacrylamide), *Sep. Purif. Technol.*, 68 (2009) 417–421.
- [17] N.S. Kwak, Y. Baek, T.S. Hwang, The synthesis of poly(vinylphosphonic acid-co-methacrylic acid) microbeads by suspension polymerization and the characterization of their indium adsorption properties, *J. Hazard. Mater.*, 203 (2012) 213–220.
- [18] F.J. Alguacil, F.A. Lopez, O. Rodriguez, S. Martinez-Ramirez, I. Garcia-Diaz, Sorption of indium (III) onto carbon nanotubes, *Ecotoxicol. Environ. Saf.*, 130 (2016) 81–86.
- [19] E. Onsøyen, Ø. Skaugrud, Metal recovery using chitosan, *J. Chem. Technol. Biotechnol.*, 49 (1990) 395–404.
- [20] E. Guibal, T. Vincent, R. Navarro, Metal ion biosorption on chitosan for the synthesis of advanced materials, *J. Mater. Sci.*, 49 (2014) 5505–5518.
- [21] H. Yan, J. Dai, Z. Yang, H. Yang, R. Cheng, Enhanced and selective adsorption of copper (II) ions on surface carboxymethylated chitosan hydrogel beads, *Chem. Eng. J.*, 174 (2011) 586–594.
- [22] W.S. Wan Ngah, K.H. Liang, Adsorption of gold (III) ions onto chitosan and N-carboxymethyl chitosan: equilibrium studies, *Ind. Eng. Chem. Res.*, 38 (1999) 1411–1414.
- [23] J. Dai, H. Yan, H. Yang, R. Cheng, Simple method for preparation of chitosan/poly(acrylic acid) blending hydrogel beads and adsorption of copper(II) from aqueous solutions, *Chem. Eng. J.*, 165 (2010) 240–249.
- [24] H. Yan, L. Yang, Z. Yang, H. Yang, A. Li, R. Cheng, Preparation of chitosan/poly(acrylic acid) magnetic composite microspheres and applications in the removal of copper(II) ions from aqueous solutions, *J. Hazard. Mater.*, 229 (2012) 371–380.
- [25] N. Li, R. Bai, Highly enhanced adsorption of lead ions on chitosan granules functionalized with poly(acrylic acid), *Ind. Eng. Chem. Res.*, 45 (2006) 7897–7904.
- [26] U.Y. Nayak, S. Gopal, S. Mutalik, A.K. Ranjith, M.S. Reddy, P. Gupta, N. Udupa, Glutaraldehyde cross-linked chitosan microspheres for controlled delivery of zidovudine, *J. Microencapsulation*, 26 (2009) 214–222.
- [27] V.K. Mourya, N.N. Inamdar, A. Tiwari, Carboxymethyl chitosan and its applications, *Adv. Mater. Lett.*, 1 (2010) 11–33.
- [28] M.V. Lopez-Ramon, F. Stoeckli, C. Moreno-Castilla, F. Carrasco-Marin, On the characterization of acidic and basic surface sites on carbons by various techniques, *Carbon*, 37 (1999) 1215–1221.
- [29] Z. Yang, H. Yang, Z. Jiang, T. Cai, H. Li, H. Li, A. Li, R. Cheng, Flocculation of both anionic and cationic dyes in aqueous solutions by the amphoteric grafting flocculant carboxymethyl chitosan-graft-polyacrylamide, *J. Hazard. Mater.*, 254 (2013) 36–45.
- [30] S.G. Wang, X.F. Sun, X.W. Liu, W.X. Gong, B.Y. Gao, N. Bao, Chitosan hydrogel beads for fulvic acid adsorption: behaviors and mechanisms, *Chem. Eng. J.*, 142 (2008) 239–247.
- [31] A.S. Michaels, O. Morelos, Polyelectrolyte adsorption by kaolinite, *Ind. Eng. Chem.*, 47 (1955) 1801–1809.
- [32] S.A. Wood, I.M. Samson, The aqueous geochemistry of gallium, germanium, indium and scandium, *Ore Geol. Rev.*, 28 (2006) 57–102.
- [33] S. Malamis, E. Katsou, A review on zinc and nickel adsorption on natural and modified zeolite, bentonite and vermiculite: examination of process parameters, kinetics and isotherms, *J. Hazard. Mater.*, 252 (2013) 428–461.
- [34] F. Wang, J. Zhao, F. Pan, H. Zhou, X. Yang, W. Li, H. Liu, Adsorption properties toward trivalent rare earths by alginate beads doping with silica, *Ind. Eng. Chem. Res.*, 52 (2013) 3453–3461.
- [35] I. Langmuir, The adsorption of gases on plane surfaces of glass, mica and platinum, *J. Am. Chem. Soc.*, 40 (1918) 1361–1402.
- [36] H.M.F. Freundlich, Über die adsorption in lasungen, *Z. Phys. Chem.*, 57 (1906) 385–470.
- [37] Y. Vijaya, S.R. Popuri, V.M. Boddu, A. Krishnaiah, Modified chitosan and calcium alginate biopolymer sorbents for removal of nickel (II) through adsorption, *Carbohydr. Polym.*, 72 (2008) 261–271.
- [38] P. Bermejo-Barrera, N. Martinez-Alfonso, A. Bermejo-Barrera, Separation of gallium and indium from ores matrix by sorption on Amberlite XAD-2 coated with PAN, *Fresenius J. Anal. Chem.*, 369 (2001) 191–194.

- [39] J.S. Liu, H. Chen, X.Y. Chen, Z.L. Guo, T.C. Hu, C.P. Liu, Y.Z. Sun, Extraction and separation of In (III), Ga (III) and Zn (II) from sulfate solution using extraction resin, *Hydrometallurgy*, 82 (2006) 137–143.
- [40] T. Yuan, J. Liu, S. Yao, H. Li, W. Xu, Synthesis of coated solvent impregnated resin for the adsorption of indium (III), *Hydrometallurgy*, 101 (2010) 148–155.
- [41] S.Y. Lagergren, Zur theorie der sogenannten adsorption gelöster stoffe, *Kungliga Svenska Vetenskapsakademiens, Handlingar*, 24 (1898) 1–39.
- [42] Y.S. Ho, G. Mckay, Kinetic models for the sorption of dye from aqueous solution by wood, *Process Saf. Environ. Prot.*, 76 (1998) 183–191.
- [43] X. Li, Y. Li, Z. Ye, Preparation of macroporous bead adsorbents based on poly(vinyl alcohol)/chitosan and their adsorption properties for heavy metals from aqueous solution, *Chem. Eng. J.*, 178 (2011) 60–68.
- [44] M.J. Jaycock, G.D. Parfitt, *Chemistry of Interfaces*, Ellis Horwood Limited, Chichester, 1981.
- [45] J. Ma, Y. Jia, Y. Jing, Y. Yao, J. Sun, Kinetics and thermodynamics of methylene blue adsorption by cobalt-hectorite composite, *Dyes Pigm.*, 93 (2012) 1441–1446.